Proceedings Paper:
Hernandez-Aquino, R, Zaidi, SAR, McLernon, D et al. (2016) Modelling and performance evaluation of non-uniform two-tier cellular networks through Stienen model. In: 2016 IEEE International Conference on Communications, ICC 2016. 2016 International Conference on Communications, 22-27 May 2016 IEEE. ISBN: 9781479966646. EISSN: 1938-1883.

https://doi.org/10.1109/ICC.2016.7511120

Modelling and Performance Evaluation of Non-Uniform Two-tier Cellular Networks through Stienen Model

Raul Hernandez-Aquino[1], Syed Ali Raza Zaidi[1], Desmond McLernon[1] and Mounir Ghogho[1,2]
[1]University of Leeds, UK
[2]International University of Rabat, Morocco
emails: {elrha, s.a.zaidi, d.c.mclernon, m.ghogho}@leeds.ac.uk

***Abstract*—In this paper we introduce Stienen's model for analysing the performance of a non-uniform two-tier networks. The topology of the network consists of a set of macro base stations (MBSs) uniformly deployed, and a set of femtocell access points (FAPs) deployed only outside exclusion areas (discs) surrounding the MBSs. The MBSs serve users within the innermost areas of each macrocell, while the femtocells are restricted to serve users located in the outermost areas towards the edge of the macrocells. Results show that the edge user performance in terms of coverage is highly increased by the addition of femtocells. Moreover, the coverage in the macrocell tier can be also increased in comparison with a macrocell-only network if the number of femtocells deployed is judiciously selected. Furthermore, a well balanced network can be achieved, where the same performance is expected throughout the entire area.**

I. Introduction

THE exponential increase in both the number of users of cellular systems and their bandwidth requirements, has created the need to increase the data rates that the system can handle and improve the coverage where it is needed. A promising solution for Next Generation Networks (NGNs) to cope with the demands for better coverage and higher data rates is the deployment of heterogeneous networks (HetNets) which consists of smaller, cheaper and less energy consuming base stations (BSs) such as femtocell access points (FAPs) overlaid with the traditional macro base station (MBS) network [1]. The use of HetNets has the potential to provide both the required coverage and increase the data rates of the users.

While femtocells were firstly considered as user deployed devices, the trend over the past years has shifted to an operator perspective due to the potential gains that are foreseen when network operators place femtocells in areas where the required QoS cannot be provided otherwise. While the typical assumption in the modelling of HetNets via Poisson point processes (PPPs) has been to consider a uniform deployment of several tiers of BSs across the area of service, this assumption lacks the notion of smart and efficient deployment, as areas close to the MBSs are expected to have higher performance in comparison with areas close to the edges of macrocells. Moreover, it is well established that traditionally the bottleneck of the cellular system resides in the edge user performance. Hence, a non-uniform deployment of femtocells, with more femtocells towards the edge of the macrocells, yields important gains in the cell edge user performance, but also creates a challenge in analytically analysing the performance of the network, due to the location dependency of the FAPs.

A non-uniform deployment of base stations among different tiers in a HetNet allows to model in a more realistic manner the behaviour of an actual network, where the positions of the base stations in different tiers are not independent. In [2], a non-uniform deployment of a heterogeneous network is proposed where 4 tiers (each one modeled by a PPP) are deployed in the area. In this model, in the fist stage a Voronoi tesselation is created with the points generated by the PPP of tier 1. Then, all the points of tiers 2 and 3 are restricted to the edges and vertices (respectively) of the Voronoi cells of tier 1. By varying the parameters and intensities of the respective PPPs, different cases of interest are pointed out and, the cell sizes as well as the effective received power in the area are presented after a series of simulations. In [3] the coverage and throughput are analysed for a two-tier networks consisting of macro- and femtocells. Both, MBSs and FAPs are uniformly deployed across the area. However, only femtocells which are located outside a circular area surrounding each MBS are activated. The paper assumes a fixed size exclusion disc surrounding each MBS and a highest instantaneous received power association scheme. In [4] a two-tier HetNet consisting of macro and pico cells is considered. The MBS tier follows a PPP, while the picocell tier follows a Poisson hole process (PHP). Therefore, the picocells are only deployed in the locations outside circular areas surrounding the MBSs with a fixed radius of exclusion. By assuming a fixed position from a typical macrocell user to its designed MBS and a typical femtocell user to its tagged pico BS, bounds on the coverage probabilities for both users are obtained.

In this paper we introduce Stienen's model for the deployment of a two-tier HetNet where we assume a deployment in which femtocells are overlaid with a MBS cellular system and placed only in areas outside discs surrounding the MBSs. In contrast with other works, we consider a dependency of the

This work was supported by CONACYT, Mexico

disc, with the size of the macrocell to which it belongs. Using well-established tools from stochastic geometry theory we model the positions of the BSs in the system via independent PPPs and obtain tractable expressions for the coverage of both tiers.

The rest of the paper is organized as follows. Section II introduces the system model. The coverage probability for the proposed model is obtained in III. The numerical results are presented in Section IV. Finally, conclusions are given in Section V.

Throughout the paper the following notations are used. The notation $E[X]$ is used to express the expected value of the random variable X. A random variable X following a complex Gaussian distribution with mean μ and variance σ^2 is expressed as $X \sim \mathcal{CN}(\mu, \sigma^2)$. A Poisson distribution with mean μ is expressed as $\text{Pois}(\mu)$, and an exponential distribution with mean μ is written as $\text{Exp}\left(\frac{1}{\mu}\right)$. Finally $\mathcal{B}(x, D)$ represents the ball of radius D centered at x.

II. System model

Consider an interference limited (the effect of noise is neglected) two tier network consisting of MBSs and FAPs deployed in a given area. The MBSs are deployed across the entire area following a PPP Φ_m, with density λ_m. The FAPs are only deployed outside the discs of radii R_s^j surrounding the MBSs, $(x^j \in \Phi_m)$ [1]. The femtocell tier is then modelled via a PHP with effective intensity $\lambda_f p$, where λ_f is the original intensity of femtocells, while p is the probability that a FAP will be located outside the above-mentioned discs of radii R_s^j, $\forall\, x_j \in \Phi_m$. In this model, the users that fall within the area covered by the discs will be served by the corresponding MBS. On the other hand, the users located outside the discs will be served by the femtocell tier. The advantages of this model are twofold: deploying femtocells only in areas where the coverage is expected to be low (near the edges of the macro cells), and improving the expected macrocell performance, since the users served by the macrocell tier will be close to their serving MBS. We assume that in both tiers, each user is associated with the closest BS. Under these assumptions, the resulting association scheme is formed by two Voronoi tessellations [5], i.e. one corresponding to the macrocell tier and the other one for the femtocell tier.

In contrast with previous works, in this paper we propose the use of Stienen's model to characterize the size of the macrocell coverage area, matching it with the area enclosed in the Stienen cells. Stienen's model [6] is described as follows. Consider the homogeneous PPP Φ_m modelling the positions of the MBSs. The points generated by Φ_m are taken as seeds to construct a Voronoi tesellation. Now, around each point $x^j \in \Phi_m$ (each Voronoi cell seed), a sphere of diameter R_s^j equal to half of the distance to the closest neighbour (r_1) is placed. Fig. 1 shows the proposed model. We can generalize

[1]Note that we will refer to $x^j \in \Phi_m$ and $x^k \in \Phi_f$ to represent, respectively, the position of the j-th and k-th points. On the other hand, we will use $j \in \Phi_m$ and $k \in \Phi_f$ with $j = 0, 1, ..., |\Phi_m|$ and $k = 0, 1, ..., |\Phi_f|$ to represent respectively, the j-th and k-th BS index.

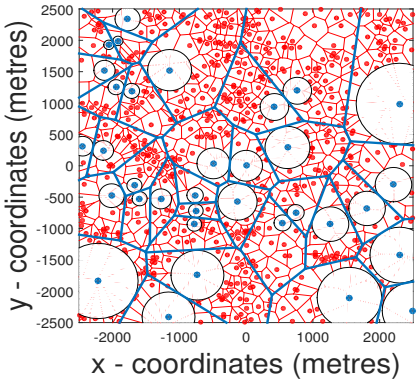

Fig. 1: Stienen's two tier network model. The blue dots represent the MBS while the red dots represent the FAPs. The blue and red lines represent respectively, the boundaries of the macrocells and femtocells coverage regions. The discs surrounding the MBS represent the Stienen's cells.

the model by considering the radius to be a linear function of the closest neighbour, i.e., $\tau\, r_1$, with $\tau > 0$. Due to the independence property of the PPP, the set of Stienen radii $\{R_s^j\} \in \Phi_m$ are all i.i.d. Therefore, we will refer to the Stienen radius only as R_s in the rest of the paper.

To model the location dependent femtocells, the FAPs with density λ_f are placed uniformly only in areas outside the Stienen cells. It is well-known that the distance of the typical user to its closest neighbour r_1 in a PPP follows a Rayleigh distribution [7]. Given that in this work it is assumed that $R_s = \tau r_1$, we can obtain the distribution of the radius of the Stienen cell as

$$f_{R_s}(R_s) = 2\pi\lambda_m R_s \tau^{-2}\, e^{-\pi\lambda_m \left(\frac{R_s}{\tau}\right)^2}. \tag{1}$$

Lemma 1. *Under Stienen's model for cellular systems, the effective density of femtocells is $\lambda_f p$, where*

$$p = \left(1 + \tau^2\right)^{-1}. \tag{2}$$

Proof. In a PHP with fixed value of an exclusion region radius R_s, for each point $x^j \in \Phi_m$, all points of $\Phi_f \bigcap \mathcal{B}(x^j, R_s)$ are removed. In this case the effective intensity of the femtocell tier is given as $\lambda_f p$, where $p = e^{-\lambda_m \pi R_s^2}$, [8]. Now, as R_s is a random variable in the proposed model, the value of p transforms into $p = E_{R_s}\left[e^{-\lambda_m \pi R_s^2}\right]$. By taking the expectation using the pdf found in (1), the expression in (2) is obtained. □

The propagation model considered is assumed to be a composite of Rayleigh flat-fading channel and path loss. For the flat fading component, we define $h_{j,k}$ as the channel between the j-th transmitter and the k-th receiver, with $h_{j,k} \sim \mathcal{CN}(0, 1)$. The path loss on the other hand is modelled as $l(r_{j,k}) = (r_{j,k})^{-\alpha_i}$, where $r_{j,k}$ is the distance from the j-th transmitter to the k-th user and α_i is the path loss exponent in tier i. We assume that the femtocells will be deployed outdoors by the network operator, and therefore the path loss exponents in both tiers are the same $(\alpha_m = \alpha_f = \alpha)$. The mean total

transmitted power of a base station in tier $i \in \{f, m\}$ is denoted as P_i^{tx}. Finally, it is assumed that the complex symbol $(s_{j,k})$ sent from the j-th transmitter to the k-th user satisfies, $E\left[|s_{j,k}|^2\right] = 1$.

III. Coverage

In this section we analyse the coverage achieved in each tier. Formally, the coverage probability $P_i^c(\beta)$ $(i \in \{m, f\})$ in an interference limited scenario is defined as the probability that the signal to interference ratio (SIR) is above a certain threshold (β) in the entire service area, i.e., $P_i^c(\beta) = P(SIR_i > \beta), i \in \{m, f\}$. Considering that both tiers share the same spectrum, the SIR is expressed as

$$SIR_i = \frac{P_i^{tx}|h|^2\, l\left(r_i\right)}{\sum\limits_{j\in\Phi_m} P_m^{tx}|h_{j,0}|^2\, l\left(r_{j,0}\right) + \sum\limits_{k\in\Phi_f} P_f^{tx}|h_{k,0}|^2\, l\left(r_{k,0}\right)} = \frac{P_i^{tx}|h_i|^2\, r_i^{-\alpha}}{I_{\Phi_m} + I_{\Phi_f}},\ \ i \in \{f, m\} \tag{3}$$

where r_i represents the distance from the typical user to its closest BS in tier i, I_{Φ_m} and I_{Φ_f} represent, respectively, the received interference from the macro- and femtocell tiers. For easiness of notation, from now on, we drop the 0 superscript for the interfering links to the typical user, i.e. $h_j = h_{j,0}$, $h_k = h_{k,0}$, $r_j = r_{j,0}$ and $r_k = r_{k,0}$. Using the fact that $|h|^2 \sim \mathrm{Exp}(1)$, the coverage probability is expressed as

$$\begin{aligned} P_i^c(\beta) = P(SIR_i > \beta) &= P\left(\frac{P_i^{tx}|h|^2\, r_i^{-\alpha}}{I_{\Phi_m} + I_{\Phi_f}}\right) \\ &= E_{r_i, R_s, I_{\Phi_m}, I_{\Phi_f}}\left[\exp\left(-\frac{r_i^\alpha \beta}{P_i^{tx}}\left(I_{\Phi_m} + I_{\Phi_f}\right)\right)\right] \\ &= E_{r_i, R_s}\left[\mathcal{L}_{\Phi_m}\left(s\right)\mathcal{L}_{\Phi_f}\left(s\right)\right]\Big|_{s=\frac{r_i^\alpha\beta}{P_i^{tx}}} \end{aligned} \tag{4}$$

where $\mathcal{L}_{\Phi_i}(s)$ is the Laplace transform of the i-th tier, with $i \in \{m, f\}$. To obtain the statistics for the typical user in each tier we place the center of the typical cell at the origin. As stated before, the distance from the typical user to the closest BS follows a Rayleigh distribution. Thus, we proceed to place the typical user at a distance r from the origin with $f_r(r) = 2\pi\lambda_m r\, e^{-\pi\lambda_m r^2}$, for $r > 0$. We assume that users inside Stienen's cells ($r < R_s$, where R_s is the radius of the Stienen cell) will be served by macro BSs, while those outside the cells ($r > R_s$) will be offloaded to the femtocells.

A. Macrocell coverage

Theorem 1. *The coverage probability in the macrocell tier is given in (5) (on top of next page), where $\zeta(a, b) = {}_2F_1\left(1, 1 - 2/a; 2 - 2/a; -b\right)$ is the Gauss hypergeometric function.*

Proof. From (4), the coverage probability in the macrocell tier is expressed as

$$P_m^c = E_{r_m}\left[\mathcal{L}_{\Phi_m}\left(s\right)\big|_{s=r_m^\alpha\beta}\, \mathcal{L}_{\Phi_f}\left(s\right)\big|_{s=r_m^\alpha\beta\eta}\right] \tag{7}$$

where $\eta = \frac{P_f^{tx}}{P_m^{tx}}$ represents the ratio of the transmit powers. Each Laplace transform corresponds exactly to the probability generating functional of a PPP [9]. For the considered scenario, the exact computation of the Laplace transform is not feasible. However, we obtain an approximation by following the approach taken in [10] for a fixed user location, and extend it for a random position in the service area. In Fig. 2 a sketch of the model used is presented. Under this scheme, the typical user which is located at a distance r from its serving MBS coincides with r_m, and so we have $f_{r_m}(r_m) = 2\pi\lambda_m r_m \exp(-\pi\lambda_m r_m^2)$. From Fig. 2, it is clear that the closest interferer is located always at a distance D from the typical user, and at a distance $R_s\tau^{-1}$ from the serving MBS, with R_s being the Stienen radius of the typical macrocell. Therefore, the Laplace transform of the macrocell interference is decomposed into two components, $\mathcal{L}_m = \mathcal{L}_m^D(s)\mathcal{L}_m'(s)$, where $\mathcal{L}_m^D$ denotes the Laplace transform of the closest interfering MBS and $\mathcal{L}_m'$ denotes the Laplace transform of the rest of interfering MBSs. Additionally, we define a variable $\psi = \frac{r_m}{R_s}$ which corresponds to the ratio between the distance from the typical user to its serving MBS and the Stienen radius of that MBS. Using the law of cosines with a minor simplification, we approximate D as

$$D \approx R_s\sqrt{\tau^{-2} + \psi^2}. \tag{8}$$

The Laplace transform of the closest interfering MBS can be then evaluated as

$$\begin{aligned} \mathcal{L}_{I_{\Phi_m}}^D(s) &= E_{I_{\Phi_m}}\left[\exp(-I_{\Phi_m}s)\big|_{s=r_m^\alpha\beta}\right] \\ &= E_{|h|^2}\left[\exp\left(-s|h|^2 D^{-\alpha}\right)\right] \\ &\overset{(a)}{=} E_{|h|^2}\left[\exp\left(-|h|^2\beta\left(\frac{\psi}{\left(\tau^{-2}+\psi^2\right)^{1/2}}\right)^\alpha\right)\right] \\ &= \left(1 + \beta\left(\frac{\psi}{\left(\tau^{-2}+\psi^2\right)^{1/2}}\right)^\alpha\right)^{-1}. \end{aligned} \tag{9}$$

As previously stated, the interference from the macrocell tier (others than the closest interferer) is not symmetric with respect to the typical user. In this case, an approximation is obtained by considering that the interference to the typical user comes from outside $\mathcal{B}\left(x^u, R_s(\tau^{-1} - \psi)\right)$, where x^u is the position of the user. The Laplace transform of the other interferers in the macrocell tier is then obtained as

$$\begin{aligned} \mathcal{L}_{I_{\Phi_m}}'(s) &= E_{I_{\Phi_m}}\left[\exp(-I_{\Phi_m}s)\big|_{s=r_m^\alpha\beta}\right] \\ &= E_{\Phi_m, |h_j|^2}\left[\exp\left(-s\sum_{j\in\Phi_m}|h_j|^2\, r_j^{-\alpha}\right)\right] \\ &= E_{\Phi_m, |h_j|^2}\left[\prod_{j\in\Phi_m}\exp\left(-|h_j|^2\beta\, r_m^\alpha\, r_j^{-\alpha}\right)\right] \\ &= E_{\Phi_m}\left[\prod_{j\in\Phi_m}\frac{1}{1+\beta\left(\frac{r_j}{r_m}\right)^{-\alpha}}\right] \end{aligned}$$

$$P_m^c(\beta) \approx \int_0^1 \frac{\frac{2\tau^{-2}\psi\left(1+\tau^{-2}\right)}{\left(\tau^{-2}+\psi^2\right)^2}\left(\frac{1}{1+\beta\left(\frac{\psi}{\left(\tau^{-2}+\psi^2\right)^{1/2}}\right)^{\alpha}}\right)\, d\psi}{1+\frac{\beta\tau^2\psi^{\alpha}}{\alpha/2-1}\left[\left(\tau^{-1}-\psi\right)^{2-\alpha}\,\zeta\left(\alpha,-\beta\left(\frac{\psi}{\left(\tau^{-1}-\psi\right)}\right)^{\alpha}\right)+\frac{\lambda_f p\eta(1-\psi)^{2-\alpha}}{\lambda_m}\,\zeta\left(\alpha,-\beta\eta\left(\frac{\psi}{1-\psi}\right)^{\alpha}\right)\right]} \tag{5}$$

$$P_f^c(\beta) \approx \int_0^{\infty} \frac{\left(2\lambda_m^2\lambda_f p\Delta\,\left(1+\tau^{-2}\right)\right)\frac{\lambda_m\left(2+\tau^{-2}+\frac{2\lambda_f p\Delta^2}{\lambda_m}\right)}{\left((\lambda_m+\lambda_f p\Delta^2)(\lambda_m(1+\tau^{-2})+\lambda_f p\Delta^2)\right)^2}\left(\frac{1}{1+\beta\eta^{-1}\Delta^{\alpha}}\right)\quad d\Delta}{1+\frac{\beta}{(\alpha/2-1)}\left[\zeta\left(\alpha,-\beta\right)+\frac{\lambda_m\Delta^{\alpha-2}}{\lambda_f\eta p}\,\zeta\left(\alpha,-\frac{\beta}{\eta}\Delta^{\alpha}\right)\right]} \tag{6}$$

$$\overset{(a)}{\approx}\exp\left(-2\pi\lambda_m\int_{R_s(\tau^{-1}-\psi)}^{\infty}\frac{v\,dv}{1+\left(\frac{v}{\beta^{1/\alpha}\psi R_s}\right)^{\alpha}}\right)$$
$$=\exp\left(\frac{-\lambda_m\pi\beta\psi^{\alpha}\left(\tau^{-1}-\psi\right)^{2-\alpha}R_s^2}{\alpha/2-1}\times\right.$$
$$\left.{}_2F_1\left(1,1-2/\alpha;2-2/\alpha;-\beta\left(\frac{\psi}{\tau^{-1}-\psi}\right)^{\alpha}\right)\right) \tag{10}$$

where (a) is obtained by using the probability generating functional of a PPP [9]. The Laplace transform for the femtocell tier is obtained by assuming a worst case scenario, where we have considered that the interference comes from outside $\mathcal{B}\left(x_0, R_s(1-\psi)\right)$, and so the typical user receives more interference than the one found in the scenario proposed. Under this assumption, we have that

$$\begin{aligned}\mathcal{L}_{I_{\Phi_f}}(s) &= E_{I_{\Phi_f}}\left[\exp(-I_{\Phi_f}s)\big|_{s=r_m^{\alpha}\beta\eta}\right]\\ &= E_{\Phi_f,|h_k|^2}\left[\exp\left(-s\sum_{k\in\Phi_m}|h_k|^2\,r_k^{-\alpha}\right)\right]\\ &= E_{\Phi_f,|h_k|^2}\left[\prod_{k\in\Phi_f}\exp\left(-|h_k|^2\beta\eta\,r_m^{\alpha}\,r_k^{-\alpha}\right)\right]\\ &= E_{\Phi_f}\left[\prod_{k\in\Phi_f}\frac{1}{1+\beta\eta\left(\frac{r_k}{r_m}\right)^{-\alpha}}\right]\\ &= e^{\frac{-\lambda_f\pi p\beta\eta\psi^{\alpha}(1-\psi)^{2-\alpha}R_s^2}{\alpha/2-1}\,{}_2F_1\left(1,1-\frac{2}{\alpha};2-\frac{2}{\alpha};-\beta\eta\left(\frac{\psi}{1-\psi}\right)^{\alpha}\right)}.\end{aligned} \tag{11}$$

where the final expression is found by conducting a similar analysis as the one used for the macrocells. It is worth pointing out that in (4) the expression for the coverage probability requires averaging over r_m and R_s. With the substitution $r_m = \psi R_s$, the expression can now be obtained by taking the average over R_s and ψ. We now proceed to find the pdfs of these parameters, i.e., $f_{R_s}(R_s)$ and $f_{\psi}(\psi)$. The pdf of ψ is obtained by directly using the definition of the ratio distribution as

$$f_{\psi}(\psi) = \int_{-\infty}^{\infty}|R_s|\,f_{R_s,r_m}(R_s,\psi R_s)\,dR_s$$

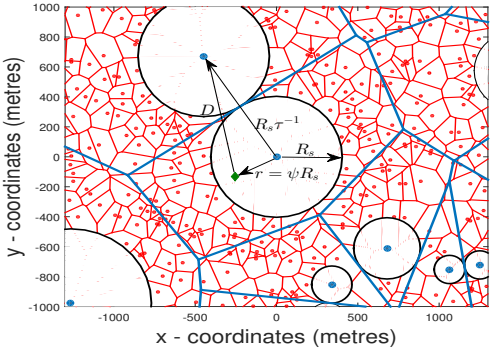

Fig. 2: Model considered for the approximation. The green diamond represents the typical user located at a distance $r = \psi R_s$ from the serving MBS, where R_s is the Stienen radius for the typical cell. The typical macrocell closest interferer is located at a distance $R_s\tau^{-1}$ from the MBS located at the origin. The distance between the user and the closest interfering MBS is denoted as D.

$$\begin{aligned}&= \int_0^{\infty} R_s \times 2\lambda_m\pi R_s\tau^{-2}\,e^{-\lambda_m\pi\left(\frac{R_s}{\tau}\right)^2}\times\\ &\quad 2\lambda_m\pi\psi R_s\tau^{-2}\,e^{-\lambda_m\pi(\psi R_s)^2}\,dR_s\\ &= 2\tau^{-2}\,\psi\left(\tau^{-2}+\psi^2\right)^{-2}.\end{aligned} \tag{12}$$

Finally, in order to effectively deal with the case when the user is served by the macrocell tier, we need to condition on the probability of the typical user being located inside the Stienen sphere $\left(p_{um} = P(x^0 \in \mathcal{B}\left(0,R_s\right)\right)$, which is equivalent to $P(\psi < 1)$. From (12) it is straightforward to obtain this probability as $p_{um} = \left(1+\tau^{-2}\right)^{-1}$. So the coverage probability in the macrocell tier is expressed as

$$P_m^c(\beta) = \frac{1}{p_{um}}\int_0^1\int_0^{\infty}\mathcal{L}^D_{I_{\Phi_m}}\mathcal{L}'_{I_{\Phi_m}}\mathcal{L}_{I_{\Phi_f}}\times$$
$$f_{R_s}(R_s)\,f_{\psi}(\psi)\,dR_s\,d\psi. \tag{13}$$

Substituting the values found in (9), (10), (11), (1) and (12) into (13) and integrating with respect to R_s, the final expression in (5) is found. □

B. Femtocell coverage

Theorem 2. *The coverage probability in the femtocell tier is given in (6) (on top of this page).*

Proof. From (4), the coverage probability in the femtocell tier is expressed as

$$P_f^c = E_{r_f}\left[\mathcal{L}_{\Phi_m}(s)|_{s=r_f^\alpha\beta\eta^{-1}}\,\mathcal{L}_{\Phi_f}(s)\big|_{s=r_f^\alpha\beta}\right]. \quad (14)$$

The Laplace transform for the femtocell interference in this case is assumed to be the same as in a normal PPP Voronoi. Therefore, the Laplace transform in this tier is given as

$$\begin{aligned}\mathcal{L}_{I_{\Phi_f}}(s) &= E_{I_{\Phi_f}}\left[\exp(-I_{\Phi_f}s)\big|_{s=r_f^\alpha\beta}\right]\\ &= E_{\Phi_f,|h_k|^2}\left[\prod_{k\in\Phi_f}\exp\left(-|h_k|^2\,r_k^{-\alpha}\beta\,r_f^\alpha\right)\right]\\ &= E_{\Phi_f}\left[\prod_{k\in\Phi_f}\frac{1}{1+\beta\left(\frac{r_k}{r_f}\right)^{-\alpha}}\right]\\ &= e^{\frac{-\lambda_f\pi\,\beta R_s^2}{\alpha/2-1}\,{}_2F_1(1,1-2/\alpha;2-2/\alpha;-\beta)}. \quad (15)\end{aligned}$$

For the macrocell tier interference, we note that the closest MBS (within the same Voronoi cell) now acts as an interferer, and it is always located at a distance r from the typical user. Similar to the case of the macrocell tier, we define a variable $\Delta = \frac{r_f}{r}$ that will help to simplify the final expression for the coverage probability. Then, the Laplace transform for the macrocell interference can again be decomposed into two Laplace transforms, i.e. $\mathcal{L}_{I_{\Phi_m}} = \mathcal{L}^r_{I_{\Phi_m}}\mathcal{L}^{''}_{I_{\Phi_m}}$, where $\mathcal{L}^r_{I_{\Phi_m}}$ corresponds to the Laplace transform of the closest interferer (at a distance r, conditioned on $r > R_s$), and $\mathcal{L}^{''}_{I_{\Phi_m}}$ is the Laplace transform of the other MBSs. The Laplace transform of the closest interferer is given as

$$\begin{aligned}\mathcal{L}^r_{I_{\Phi_m}}(s) &= E_{I_{\Phi_m}}\left[\exp(-I_{\Phi_m}s)|_{s=r_f^\alpha\beta\eta^{-1}}\right]\\ &= E_{|h|^2}\left[\exp\left(-s|h|^2r^{-\alpha}\right)\right]\\ &\overset{(a)}{=} E_{|h|^2}\left[\exp\left(-|h|^2\beta\eta^{-1}\Delta^\alpha\right)\right]\\ &= \left(1+\beta\eta^{-1}\Delta^\alpha\right)^{-1}. \quad (16)\end{aligned}$$

For the Laplace transform of the other macrocell interference, we observe that the interference can be as close as $r = \frac{r_f}{\Delta}$ (with $r > R_s$). Therefore, we have

$$\begin{aligned}\mathcal{L}^{''}_{I_{\Phi_m}}(s) &= E_{I_{\Phi_m}}\left[\exp(-I_{\Phi_m}s)|_{s=r_f^\alpha\beta\eta^{-1}}\right]\\ &= E_{\Phi_m,|h_j|^2}\left[\prod_{j\in\Phi_m}\exp\left(-|h_j|^2\,r_f^\alpha\,\beta\,\eta^{-1}\,r_j^{-\alpha}\right)\right]\\ &= E_{\Phi_m}\left[\prod_{j\in\Phi_m}\frac{1}{1+\beta\eta^{-1}\left(\frac{r_j}{r_f}\right)^{-\alpha}}\right]\\ &\overset{(a)}{=}\exp\left(-2\pi\lambda_m\int_{\frac{r_f}{\Delta}}^\infty\frac{v\,dv}{1+\left(\frac{v}{\beta^{1/\alpha}\eta^{-1/\alpha}r_f}\right)^\alpha}\right)\\ &= e^{-\pi\lambda_m\left(\frac{\beta}{\eta}\right)^{2/\alpha}r_f^2\int_{\left(\left(\frac{\beta}{\Delta}\right)^{1/\alpha}\Delta\right)^{-2}}^\infty\frac{du}{1+u^{\alpha/2}}}\\ &= e^{\frac{-\lambda_m\pi\beta\eta^{-1}\Delta^{\alpha-2}r_f^2}{\alpha/2-1}\,{}_2F_1\left(1,1-2/\alpha;2-2/\alpha;-\beta\eta^{-1}\Delta^\alpha\right)} \quad (17)\end{aligned}$$

where (a) is obtained by using the PGF of a PPP. The final expression for the coverage probability needs to be averaged over Δ and r_f. The pdf of r_f is directly obtained from the closest neighbour distribution of a PPP considering the thinning probability p as

$$f_{r_f}(r_f) = 2\pi\lambda_f\,p\,r_f\exp\left(-\pi\lambda_f\,p\,r_f^2\right). \quad (18)$$

In order to obtain the pdf $f_\Delta(\Delta_)$, we first need to obtain the pdf of the distance to the closest MBS conditioned on $r > R_s$. We will denote as R the random variable following the Rayleigh distribution for the closest neighbour with the condition that it can only take values above R_s. As R_s is a random variable itself, R follows a random truncated distribution and its pdf can be found as

$$\begin{aligned}f_R(R) &= \int_0^R f\left(R|R_s\right)f(R_s)dR_s\\ &= \int_0^R 2\pi\lambda_m R\,e^{-\pi\lambda_m R^2}(2\pi\lambda_m\tau^{-2}R_s e^{-\pi\lambda_m\left(\frac{R_s}{\tau}\right)^2})dR_s\\ &= 2\pi\lambda_m R\,e^{-\pi\lambda_m R^2}\left(1-e^{-\pi\lambda_m\tau^{-2}R^2}\right). \quad (19)\end{aligned}$$

Once the distribution of R is found, the pdf of Δ can be obtained by means of the ratio distribution as

$$\begin{aligned}f_\Delta(\Delta) &= \int_{-\infty}^\infty |R|f_{R,r_f}(R,\Delta r_f)\,dR\\ &= \int_0^\infty R\;\times\;2\pi\lambda_m R\,e^{-\lambda_m\pi R^2}\left(1-e^{-\pi\lambda_m\tau-2R^2}\right)\;\times\\ &\qquad 2\pi\lambda_f\,p\,\Delta R\,e^{-\pi\lambda_f\,p\,(\Delta r_f)^2}dR\end{aligned}$$

$$\begin{aligned}&= 2\lambda_m^2\lambda_f\,p\,\tau^{-2}\Delta\;\times\\ &\left(\frac{\lambda_m\left(2+\tau^{-2}\right)+2\lambda_f\,p\,\Delta^2}{\left(\left(\lambda_m+\lambda_f\,p\,\Delta^2\right)\left(\lambda_m\left(1+\tau^{-2}\right)+\lambda_f\,p\,\Delta^2\right)\right)^2}\right). \quad (20)\end{aligned}$$

With the expressions previously obtained and conditioning on the probability of the user being served by the femtocell tier $p_{uf} = 1-p_{um}$, the femtocell coverage probability is given by

$$P_f^c(\beta) = \frac{1}{p_{uf}}\int_0^\infty\int_0^\infty\mathcal{L}^r_{I_{\Phi_m}}\mathcal{L}^{''}_{I_{\Phi_m}}\mathcal{L}_{I_{\Phi_f}}f_{r_f}(r_f)f_\Delta(\Delta)dr_f d_\Delta. \quad (21)$$

Substituting the values found in (15), (16), (17), (18) and (20) into (21) and integrating with respect to r_f, the final expression in (6) is found. □

IV. Numerical results

In this section, we validate the developed framework with Monte-Carlo simulations to explore the coverage performance for the considered HetNet deployment. Results are presented in figures 3 to 4, where circles represent the results from Monte-Carlo simulations (with 3 x 10^4 runs for each point) while lines correspond to the analytical results.

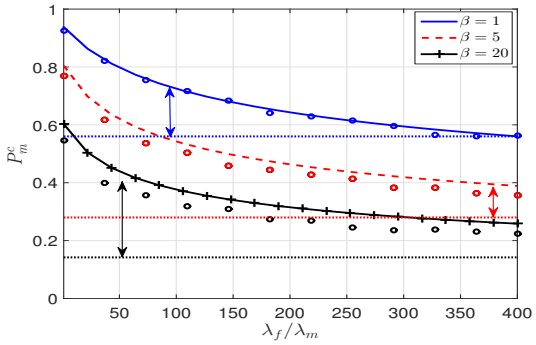

Fig. 3: Macrocell coverage probability (5) as a function of the density of femtocells deployed in the area for different threshold values β, and for $\tau = \frac{1}{2}$. The straight dotted lines correspond to the coverage probability of a single tier network with same value of β.

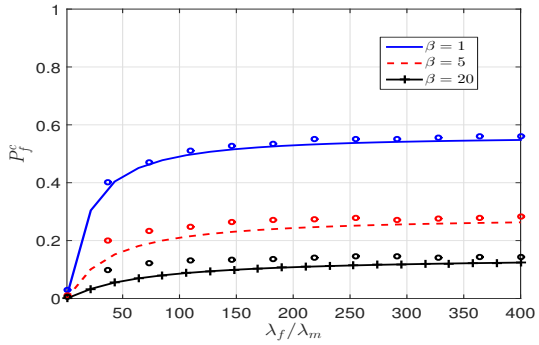

Fig. 4: Femtocell coverage probability (6) as a function of the density of femtocells deployed in the area for different threshold values β, and for $\tau = \frac{1}{2}$.

Fig. 3 shows the coverage probability in the macrocell tier, when the number of femtocells is increased in the service area. The results validate the closeness of the proposed approximation. Moreover, for a value of $\beta = 20$ the variation between the results from simulations and the analytical results is less than 5%. Additionally, for comparison purposes we have included the coverage probability (dotted straight lines) of a macrocell only network with same threshold β . The gains in the coverage probability in comparison with the traditional network can be observed. It can be seen that for the non-uniform deployment proposed, the macrocell coverage probability outperforms the traditional network even for a high number of femtocells deployed in the area. Moreover, depending upon the value of β a different number of femtocells is required for the system to reach the same performance as a traditional network.

In Fig. 4, we present the coverage probability for the femtocell tier, as a function of the femtocells density. We observe that increasing the number of femtocells in the area can increase the coverage probability for a fixed value of β. This is an expected behaviour when the interference is not very high. Moreover, when the number of femtocells deployed is high enough, the coverage probability can reach values similar to the macrocell tier. These results corroborate the initial belief that deploying femtocells in the areas towards the edge of the macrocells can improve the cell edge user performance. Moreover, when the number of femtocells deployed is high enough, the coverage probability in the femtocell tier achieves values close to those obtained in the macrocell tier. Furthermore, if the number of femtocells deployed in the area is judiciously selected, the same performance can be achieved for the femtocell and macrocell users. It can then be concluded that the proposed model can attain a uniform performance in the entire network. Note that by incorporating the strategic positioning of femtocells into the model, the coverage probability is strongly coupled to the density of BSs. This is in contrast with results from other works which consider that all tiers are uniformly distributed in the area, in which case the coverage is independent of the density of BSs [5], [11].

V. Conclusions

In this paper we introduced Stienen's model for the modeling of non-uniform network deployment. With this model, femtocells are only deployed outside discs surrounding the macro base stations. Using stochastic geometry tools we found approximations for the coverage probability of the network. Results confirm high gains in the coverage probability that can be achieved by cleverly placing femtocells in areas where the performance is expected to be low (near the edge of each MBS). Additionally, a more balanced network can be achieved. Thus, by selecting the correct number of femtocells, the same performance can be expected throughout the entire service area.

References

[1] A. Damnjanovi, J. Montojo, Y. Wei, T. Ji, T. Luo, M. Vajapeyam, T. Yoo, O. Song, and D. Malladi, "A survey on 3gpp heterogeneous networks," *IEEE Wireless Communications*, vol. 18, no. 3, pp. 10 – 21, June 2011.

[2] M. Haenggi, "A versatile dependent model for heterogeneous cellular networks," *arXiv preprint arXiv:1305.0947*, 2013.

[3] H. Wang, X. Zhou, and M. Reed, "Coverage and throughput analysis with a non-uniform small cell deployment," 2014.

[4] N. Deng, W. Zhou, and M. Haenggi, "A heterogeneous cellular network model with inter-tier dependence,," in *IEEE Global Communications Conference (GLOBECOM14)*, 2014.

[5] J. G. Andrews, F. Baccelli, and R. Krishna, "A tractable approach to coverage and rate in cellular networks," *IEEE Transactions on Communications*, vol. 59, no. 11, pp. 3122 – 3134, November 2011.

[6] V. Olsbo, *Spatial Analysis and Modelling Motivated by Nerve Fiber Patterns*. Chalmers University of Technology, 2008.

[7] M. Haenggi, "On distances in uniformly random networks," *IEEE Transactions on Information Theory*, vol. 51, no. 10, pp. 3584–3586, 2005.

[8] ——, *Stochastic Geometry for Wireless Networks*. Cambridge University Press, 2012, cambridge Books Online. [Online]. Available: http://dx.doi.org/10.1017/CBO9781139043816

[9] D. Stoyan, W. S. Kendall, and J. Mecke, *Stochastic Geometry and Its Applications*, 2nd ed. WILEY, 1995.

[10] T. Bai and R. W. Heath, "Location-specific coverage in heterogeneous networks," *Signal Processing Letters, IEEE*, vol. 20, no. 9, pp. 873–876, 2013.

[11] H. S. Dhillon, R. Krishna, F. Baccelli, and J. G. Andrews, "Modeling and analysis of k-tier downlink heterogeneous cellular networks," *Journal on Selected Areas in Communications*, vol. 30, no. 3, pp. 550 – 560, April 2012.